

Statistical Hadronization Probed by Resonances

Giorgio Torrieri and Johann Rafelski

Department of Physics, University of Arizona, Tucson, AZ 85721

(Dated: December, 2002)

Hadron freeze-out scenarios used in the analysis of (strange) hadron spectra are evaluated. We show how models follow from different physical assumptions about the freeze-out dynamics of a new state of matter such as quark gluon plasma. We find that before hadronization conditions such as temperature and/or collective matter flow can be uniquely extracted from particle spectra, the mechanism of freeze out needs to be understood. We show that the m_T dependence of ratios of spectra of hadrons with its excited resonance are sensitive to the freeze-out mechanism, allowing differentiation between statistical hadronization models. PACS: 12.38.Mh, 25.75.-q, 24.10.Pa

Introduction

The statistical model of particle production [1, 2, 3] has been used extensively to study both particle yields [4, 5, 6] and spectra. In recent years, the quality of experimental fits to statistical models was such that it became possible to get quantitative results (rather than just qualitative agreement) from them [4, 5, 6].

In particular, several analyses of SPS and RHIC particle abundances and spectra have been performed in recent years. It has become widely accepted that a model based on statistical hadronization, combined with transverse expansion, can explain both the abundances and the transverse momentum distributions of hadrons produced in heavy ion collisions.

The fitted parameters, and in particular the temperature, however, have varied considerably, ranging from as low as 110 MeV [7, 8] to 140 MeV [4, 9] to as high as 160 and 170 MeV [5, 10, 11, 12, 13].

Such discrepancies are not very surprising, since the models differ considerably. However, this means that before we can say that the freeze-out temperature has been determined, we must understand precisely the origins of these differences, and try to ascertain which model is “the best”, both in terms of physical reasonableness and as an ansatz to fit the data.

We start by giving an overview of the ways in which these models differ, and what these differences tell us about the physical assumptions used. It should be noted that every model described here gained acceptance of part of the heavy ion community; This is both because there is considerable disagreement about what the freeze-out dynamics might actually look like, and because the differences between each fit’s statistical significance are not considered to be salient enough to suggest a firm preference. For this reason, rather than engage in a comparative study of each model, we shall suggest experimental observables which will be particularly sensitive to the differences between the existing scenarios, in the hope that further experimental study will enable this ambiguity to be settled.

Firstly, spectra are normalized very differently in different models. [7, 8, 13] fit the particle slopes only, treating the normalization of each particle as a free parameter. This is consistent with the idea of a post-hadronization “interacting hadron gas phase” in which hadron abun-

dances remain approximately the same, but elastic interactions allow the system to re-equilibrate thermally. [5] and [12] introduce flavor chemical potentials, and assume the light flavours are in chemical equilibrium. The high temperature derived in these fits also makes an interacting hadron gas phase likely, making the introduction of a different thermal freeze-out temperature necessary [11]. [10] also assumes light flavour chemical equilibration, although they find that the chemical equilibration temperature also describes thermal spectra convincingly, suggesting that the re-interaction phase is short and not very significant. Finally, [9] and [4] do not assume chemical equilibrium for either light or strange flavors, and have both light and strange quark phase space occupancies $\gamma_{q,s}$ as parameters in the fit.

These different ways to describe particle yields are actually enough, by themselves, to account for the range of temperatures encountered; If the gas is not completely re-equilibrated, temperature will affect both the absolute number of particles and the spectrum. Hence, one expects that the temperature minima will change considerably if all temperature dependence of normalization is removed. Furthermore, phase space occupancy will be strongly correlated with the temperature, since the effect of both these variables on normalization will be the same for the particle and the antiparticle. [4] finds that the introduction of the phase space occupancies $\gamma_{q,s}$ lowers the fitted temperature from ~ 180 to ~ 140 MeV, and decreases the χ^2/DoF considerably.

Furthermore, some fits [7, 8, 13] do not include the contribution of resonances into the slopes, while others [9, 10] do. These approaches, consistent with the authors position on the existence of the interacting hadron gas phase (which, if it exists, should re-equilibrate the momentum distribution of resonance decay products), also account for ~ 20 MeV in the fitted temperature.

Studies discussing different approaches to chemical abundances [4] and resonance production [14] have already appeared in the literature. In particular, direct detection of resonances has been proposed as a method to distinguish between these scenarios [15], and experimental efforts in this direction are earnestly progressing [16, 17, 18, 19]. Direct detection of resonances, while helping to elucidate how resonances impact transverse mass slopes, also helps to isolate the dynamical (as op-

posed to the chemical) aspects of freeze-out, since using particles with the same quark composition makes the ratio insensitive to both fugacities and phase space occupancies.

We shall develop this approach to tackle one issue which has, as yet, not been widely discussed: The choice of freeze-out geometry. When fitting the particle spectra, the system's spatial shape and the way the freeze-out progresses in time have a considerable effect on the form of particle distributions, and hence on the fitted temperature and flow. The models used in [7, 8, 9, 10, 13] in fact all use a different choice of freeze-out geometry, based on different hadronization scenarios. The different ways the system can freeze-out and the impact of freeze-out geometry on particle spectra were examined some time before RHIC and most SPS data was available [20, 21]. For this reason, a phenomenological analysis of the different freeze-out models, to ascertain their physical significance, their ability to fit data, and possible probes capable of differentiating between them, has never been conducted.

Flow profile and the Cooper-Frye formula

Every fit quoted here uses the now standard Cooper-Frye formula [22], at most applying corrections to it [23, 24]. The truncated Cooper-Frye formula used hence forward is:

$$E \frac{dN}{d^3p} = \int p^\mu d^3\Sigma_\mu f(p^\mu u_\mu, T, \lambda) \theta(p^\mu d^3\Sigma_\mu) \quad (1)$$

Where

- p^μ is the particle's four-momentum
- u^μ is the system's velocity profile
- T is the temperature
- λ is a chemical potential
- $f(E, T, \lambda)$ is the statistical distribution of the emitted particles in terms of energy and conserved quantum numbers
- Σ^μ describes the hadronization geometry; It is the covariant generalization of a volume element of the fireball: A “3-D” surface in spacetime from which particles are emitted.
- $\theta(p^\mu d^3\Sigma_\mu)$ is the step function, which corrects inward emission [23, 24]

The Cooper-Frye formula is the most general way to implement statistical emission of particles [20, 25]. For it to represent a physical description of the system, two conditions have to be met:

Firstly, Statistical Hadronization must apply; The particles emitted from a volume element (in its comoving frame), will be distributed according to the Bose-Einstein or Fermi-Dirac distributions $f(E, T, \lambda)$ for some temperature T and fugacity λ .

Secondly, a “small” volume element hadronizes quickly in its rest frame. (in other words, no long mixed QGP-hadronic phase exists). If this condition is satisfied, it becomes possible to define a Hadronization hypersurface $\Sigma^\mu = (t_f(x, y, z), x, y, z)$ which describes the time t_f at which point (x, y, z) emits hadrons. The properties of Σ^μ can be understood by realizing that it is the covariant generalization of the number of particles produced by a volume element

$$dN = \rho dV \quad (2)$$

Relativistically, since the density ρ is part of the current 4-vector j^μ , the volume will need to be generalized to a 4-vector element, with each component having dimensions of volume.

$$dN = j^\mu d^3\Sigma_\mu \quad (3)$$

where $d^3\Sigma^\mu$ points into the direction “perpendicular to the volume element” (purely timelike, in case of eq. 2)

If a long mixed phase does exist, it might well be that the Cooper-Frye formula can be used as an approximation technique to transform a hydrodynamical system into hadrons (indeed, authors who believe in a long mixed phase have done so [26]). However, it is only in the fast hadronization case that Σ^μ describes a physically significant concept. If this is the case, different choices of the freezeout surface correspond to physically different scenarios, and it becomes possible, in principle, to distinguish them experimentally. In the next section, we explore a few of these scenarios, to see whether such distinction can also be made in practice.

Hadronization hypersurfaces

A general 3-dimensional hypersurface Σ^μ in 4-dimensional Minkowski space can always be described in terms of three independent parameters u, v, w . We can then obtain, in terms of these parameters, three independent line elements tangent to the hypersurface.

$$d^3\Sigma_u^\mu = \Sigma^\mu(u + \delta u) - \Sigma^\mu(u) = \frac{\partial \Sigma^\mu}{\partial u} du \quad (4)$$

$$d^3\Sigma_v^\mu = \frac{\partial \Sigma^\mu}{\partial v} dv \quad (5)$$

$$d^3\Sigma_w^\mu = \frac{\partial \Sigma^\mu}{\partial w} dw \quad (6)$$

The individual hypersurface element $d^3\Sigma^\mu$, can be represented by the vector perpendicular to all the vectors in Eq. 4-6. This is given by

$$d^3\Sigma_\mu = -\epsilon_{\mu\nu\lambda\eta} \frac{\partial \Sigma^\nu}{\partial u} \frac{\partial \Sigma^\lambda}{\partial v} \frac{\partial \Sigma^\eta}{\partial w} du dv dw \quad (7)$$

(The minus sign ensures $d^3\Sigma_\mu$ is future-pointing).

While an arbitrary system's freeze-out hypersurface will in general be of arbitrary shape (determined by initial conditions and hydrodynamic evolution), we are interested in studying how the freeze-out dynamics impacts on the form of $d^3\Sigma_\mu$. For this reason, we will concentrate on

limiting cases (for instance, perfectly central collisions) with a high degree of symmetry. We will then exploit this symmetry (invariance under rotations or boosts) in our choice of parameters, and see how qualitatively different choices of Σ^μ impact the form of eq. 1.

In presence of a high baryon stopping, it might be reasonable to describe emission at mid-rapidity through an approximately spherical source. It is then convenient to write Σ^μ in spherical coordinates.

$$\Sigma^\mu = (t_f, r \sin(\theta) \cos(\phi), r \sin(\theta) \sin(\phi), r \cos(\theta)). \quad (8)$$

Spherical symmetry is imposed by requiring t_f to only depend on r . Hence, by using $(u, v, w) \rightarrow (r, \theta, \phi)$, $d^3\Sigma^\mu$ can be computed, and found, not surprisingly, to be oriented in the radial direction in space [20].

$$d^3\Sigma^\mu = (1, \frac{\partial t_f}{\partial r} \vec{e}_r) d^3r \quad (9)$$

Such a surface, together with the Cooper-Frye formula, gives the hyperon distribution considered in [9]. We found that it provides a good fit to SPS data.

As the collision energy increases, however, the system conditions approach the Bjorken picture [27], and boost-invariance becomes the dominant symmetry on which freeze-out geometry should be based. To construct such a hadronization scenario, we consider the most general particle momentum and flow profile, where the Longitudinal (last) coordinate is defined along the beam direction.

$$u^\mu = \begin{pmatrix} \cosh(y_L) \cosh(y_T) \\ \sinh(y_T) \cos(\theta) \\ \sinh(y_T) \sin(\theta) \\ \sinh(y_L) \cosh(y_T) \end{pmatrix}, p^\mu = \begin{pmatrix} m_T \cosh(y) \\ p_T \cos(\phi) \\ p_T \sin(\phi) \\ m_T \sinh(y) \end{pmatrix} \quad (10)$$

Hence, the rest energy used in the Cooper-Frye formula goes as [28]

$$p_\mu u^\mu = m_T \cosh(y_T) \cosh(y - y_L) - \sinh(y_T) \cos(\theta - \phi) p_T \quad (11)$$

The requirement for the Bjorken picture is that the emission volume element has the same y_L dependence.

$$p_\mu d^3\Sigma^\mu \sim A \cosh(y - y_L) + B \quad (12)$$

This constrains the freeze-out hypersurface to be of the form

$$\Sigma^\mu = (t_f \cosh(y_L), x, y, t_f \sinh(y_L)) \quad (13)$$

Where t_f is a parameter invariant under boosts in the z direction, whose physical significance depends on the model considered.

It will then be possible to enforce boost-invariance by assuming each unit of rapidity y_L carries a fireball comoving with it. The total particle distribution will then be given by

$$E \frac{dN}{d^3p} (m_T, y_T, \theta, \phi) = \int_{-\infty}^{\infty} dy_L h(y - y_L) f(p^\mu u_\mu) \quad (14)$$

$$h(y - y_L) = p^\mu d^3\Sigma_\mu$$

For central collisions, a further simplifying constraint is provided by the cylindrical symmetry, which forces t_f , as well as y_L and y_T to be independent of the angles θ and ϕ . The freeze-out hypersurface can be parametrized, in this case, as

$$\Sigma^\mu = (t_f(r) \cosh(y_L), r \sin(\theta), r \cos(\theta), t_f(r) \sinh(y_L)) \quad (15)$$

Parametrizing Σ^μ with $u, v, w \rightarrow r, \theta, y_L$ we get the hadronization hypersurface

$$d^3\Sigma^\mu = t_f r dr d\theta dy_L \begin{pmatrix} \cosh(y_L) \\ \frac{\partial t_f}{\partial r} \cos(\theta) \\ \frac{\partial t_f}{\partial r} \sin(\theta) \\ \sinh(y_L) \end{pmatrix} \quad (16)$$

And an emission element

$$p^\mu d^3\Sigma_\mu = t_f r dr d\theta dy_L [m_T \cosh(y - y_L) - p_T \frac{\partial t_f}{\partial r} \cos(\theta - \phi)] \quad (17)$$

with the same dependence on the angle as Eq. 11. The Cooper-Frye formula can then be integrated over all the possible values of y_L and $\theta - \phi$ to give a particle spectrum depending purely on the transverse mass, temperature and y_T . The fits in [7, 8, 13] and [10] are based on such an Ansatz.

What distinguishes the models currently on the market is the time component of the freeze-out surface. The most general freeze-out hypersurface compatible with cylindrical symmetry is provided by Eq. 15. Generally, t_f (a generic function of r) represents the time, in a frame comoving with the longitudinal flow, at which the surface at distance r freezes out.

The fits in [7] and [8, 13] are based on a particular case of such a freeze-out surface, in which t_f is completely independent of r ($\frac{\partial t_f}{\partial r} = 0$). Such a picture's fundamental physical reasonableness is doubtful (why should spatially distant volume elements, presumably with different densities and moving at different transverse velocities, all freeze out simultaneously in a longitudinally comoving frame?) but it can perhaps serve as a good approximation. In particular, this model might be similar to the “explosive hadronization” envisioned by some authors [30, 31].

A more general model is to assume that emission occurs through a 3-D surface (“hadronization surface”) moving with time to at a constant “velocity” ($\frac{\partial t_f}{\partial r} = \text{constant}$, to be fitted) throughout the fireball.

This “blast wave model” is the boost-invariant analogue to the model used in [9]. While it adds an extra parameter on which the spectra depend (Temperature, flow velocity, and now $\frac{\partial t_f}{\partial r}$), it is worth considering since it is based on a very physically reasonable picture. In particular, the blast wave picture is the most compatible with sudden hadronization models. In these scenarios, hadronization occurs when the fireball encounters a

mechanical instability at the point in which the momentum flux of the expanding fireball at the QGP-vacuum boundary is balanced by the vacuum pressure [29]. The mechanical instability, combined with the fireball's high transverse flow, ensures that the emission surface spreads to the interior of the fireball with a speed comparable to c . ($\frac{\partial t_f}{\partial r} \sim 1$). All of the indications suggested for such a picture seem to be borne out by both SPS and RHIC data [4, 29, 32].

Finally, one can assume that each element of the system undergoes freeze-out at the same proper time τ . It would mean that t_f in Eq. 15 is equal to $\tau \cosh(y_T)$ and the hadronization hypersurface in Eq. 17 becomes proportional to the flow vector

$$\Sigma^\mu = \tau u^\mu \quad (18)$$

$$d^3\Sigma^\mu = \tau r dr d\theta dy_L u^\mu \quad (19)$$

$$r = \tau \sinh(y_T) \quad (20)$$

Such a scenario (In which, the cooper-Frye formula reduces to the Touscheck approach [34, 35]) follows from a hadronization model which has the heavy ion fireball behaving similarly to the expanding universe. If this model is correct, dynamical effects due to expansion and pressure from the external vaccuum play little role in the phase transition; As time moves forward, each fireball element expands and cools down independently, hadronizing when it's temperature and density reach the critical value. This ansatz was fitted to RHIC data in [10].

If the $\Theta(p^\mu d^3\Sigma_\mu)$ correction in Eq. 1 is negligible (It is only relevant for Blast-type freeze-out, when the emission surface moves considerably more slowly than the speed of light, $\frac{\partial t_f}{\partial r} \gg \frac{1}{v_T}$. HBT and fits strongly disfavor such a picture [30, 32]), and in the Boltzmann limit, it is possible to perform the integrals over the longitudinal rapidity and angle analytically using the I and K modified Bessel functions.

$$I_n(z) = \frac{1}{\pi} \int_0^\pi \cos(ny) e^{-z \cos(y)} dy \quad (21)$$

$$K_n(z) = \int_0^\infty \cosh(ny) e^{-z \cosh(y)} dy \quad (22)$$

Table I and Fig. 1 summarize the freeze-out scenarios examined here, while Fig 2 compares different freeze-out geometries for the same temperature and flow. It is apparent that the choice of freeze-out geometry produces a non-trivial effect capable of altering significantly the statistical hadronization parameters.

It is therefore imperative that we investigate if the present data can provide further ways to differentiate between the freeze-out models under consideration.

An obvious indication of whether the spherical or the boost-invariant approximations are most appropriate are the particle rapidity distributions. SPS rapidity distributions for measured hadrons [36, 37, 38], especially

antibaryons and hyperons, do not show a strong mid-rapidity peak, making the spherical freezeout Ansatz for a fit to hyperon distributions reasonable. The same, however, can not be said of RHIC, where pseudorapidity and rapidity distributions available suggest a flat peak spanning a roughly two units around mid-rapidity. [39, 40]. While it will be interesting to see whether heavier baryons (in particular hyperons and antihyperons) maintain a similar dependence, it is reasonably safe to assume that the boost-invariant limit is a better approximation for RHIC. Further distinguishing between the Hubble and different Blast-type models can in principle be done using a simultaneous fit to particle spectra. However, such a fit will exhibit a lot more sensitivity to temperature and flow than to the freeze-out model, since $E \frac{dN}{d^3p}$ depends exponentially on $p_\mu u^\mu$ and only linearly on $p_\mu d^3\Sigma^\mu$. Given this, the ambiguity present in past fits is perhaps not so surprising.

We have performed an analysis of SPS hyperon spectra using the spherical freeze-out ansatz [9], finding that χ^2 fits favor a Blast-type model with the freezeout hypersurface moving at the speed of light. (with an acceptable minimum in the χ^2 profile w.r.t. $\frac{\partial t_f}{\partial r}$) We are in the process of carrying out a similar study at RHIC energy, but the fact that all of the models described previously lead to more or less statistically reasonable fits casts doubt on the feasibility of obtaining an unambiguous picture of freezeout dynamics from the particle spectra alone. To enhance the sensitivity of experimental data to the freeze-out model, it is best to look for experimental observables in which the stronger exponential dependence cancels out. Resonance ratios might provide us with such an observable.

momentum dependance of the resonance ratios as a Freeze-out probe

In the past, we have argued that the direct measurement of resonances can probe both the hadronization temperature and the lifetime of the interacting hadron gas phase. [14, 15]. Ratios of a generic resonance (henceforward called Y^*) to the light particle (which we'll refer to as Y) with an identical number of valence quarks are particularly sensitive freezeout temperature probes because all chemical dependance cancels out within the ratio. If we examine this ratio within an m_T range in which both Y and Y^* are present, we naively expect most temperature dependance to cancel out as well, leaving us with a probe mainly sensitive to flow and the freezeout conditions.

We therefore take the most general Boost-invariant freeze-out hypersurface in the Boltzmann limit (Table I)

$$\frac{dN}{dm_T^2} \propto S(m_T, p_T, \alpha, \beta) \quad (23)$$

$$S(m_T, p_T, \alpha, \beta) = m_T K_1(\beta m_T) I_0(\alpha p_T) - \frac{\partial t_f}{\partial r} p_T K_0(\beta m_T) I_1 \quad (24)$$

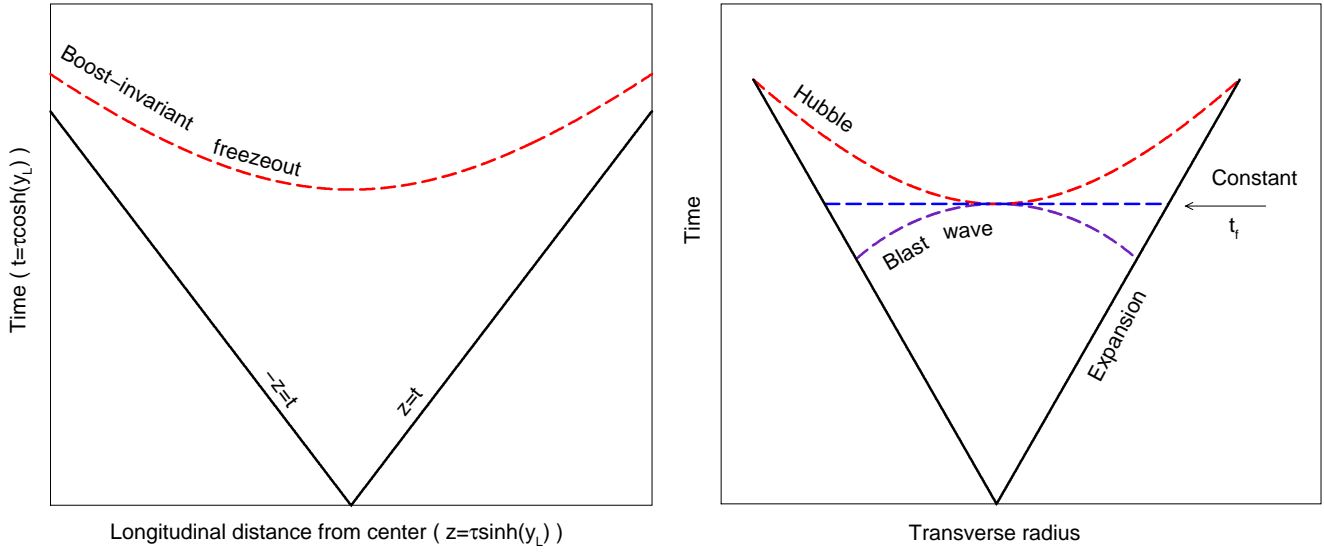


FIG. 1: While boost-invariance fixes the longitudinal freeze-out structure, several scenarios exist for the transverse dependence of freeze-out. For spherical freeze-out, only plot on the right applies

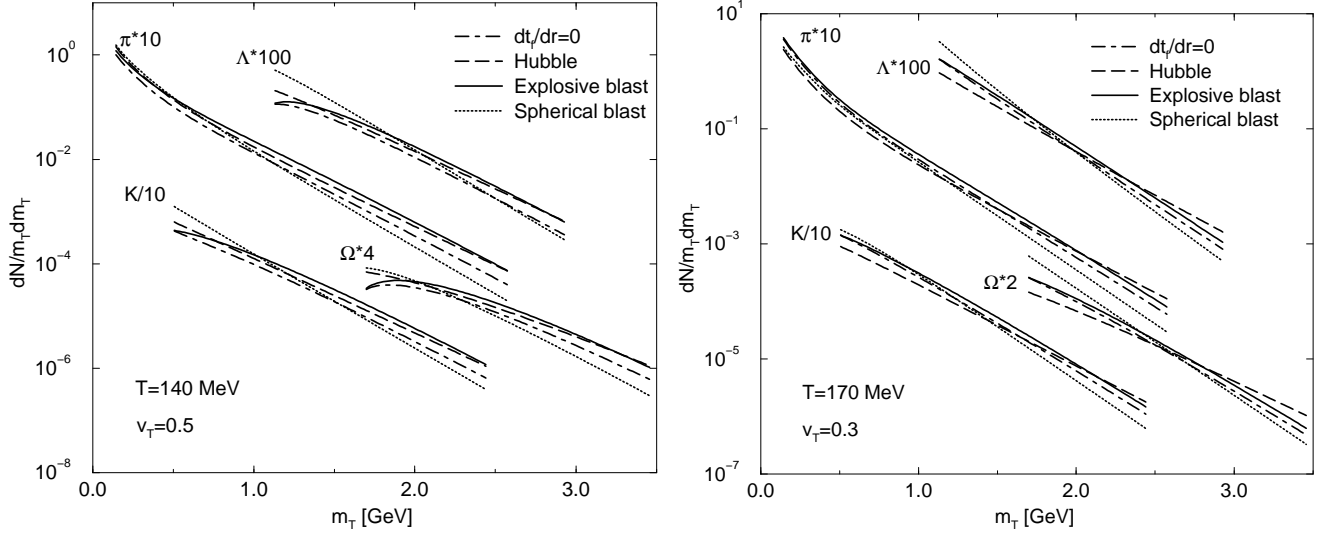


FIG. 2: π, K, Λ and Ω m_T distributions with different freezeout models

$$\beta = \frac{\cosh(y_T)}{T} \quad (25)$$

$$\alpha = \frac{\sinh(y_T)}{T} \quad (26)$$

and use it to calculate the ratio between two particles with the same chemical composition. The chemical factors cancel out, and we are left with

$$\frac{Y^*}{Y} = \left(\frac{g^*}{g} \right) \frac{S(m_T, p_T^*, \alpha, \beta)}{S(m_T, p_T, \alpha, \beta)} \quad (27)$$

Where g^* and g refers to each particle's degeneracy and the function $S(m_T, p_T, \alpha, \beta)$ is given by eq. 24. (Note that m_T is the same for Y^* and Y , but p_T varies). We note, furthermore, that for all cases considered m_T is

significantly larger than the Temperature. We recall the leading term in the asymptotic exponential of the modified bessel function

$$K_\nu(z) \approx \frac{e^{-z}}{\sqrt{2\pi z}} \quad (28)$$

If only this leading term is considered, all dependence on β of the ratio cancels out, and we are left with

$$\frac{Y^*}{Y} = \left(\frac{g^*}{g} \right) \frac{m_T I_0(\alpha p_T^*) - \frac{\partial t_f}{\partial r} p_T^* I_1(\alpha p_T^*)}{m_T I_0(\alpha p_T) - \frac{\partial t_f}{\partial r} p_T I_1(\alpha p_T)} \quad (29)$$

Eqn. 29 depends only on two parameters $\alpha = \frac{v \gamma_T}{T}$ and $\frac{\partial t_f}{\partial r}$ both of which can be extracted from a single fit.

Similarly, in case of the spherically symmetrical freeze-out scenario, the momentum dependance of the particle ratios becomes [20]

$$\frac{Y^*}{Y} = \left(\frac{g^*}{g} \right) \frac{m_T I_{1/2}(\alpha p_T^*) - \frac{\partial t_f}{\partial r} p_T^* I_{3/2}(\alpha p_T^*)}{m_T I_{1/2}(\alpha p_T) - \frac{\partial t_f}{\partial r} p_T I_{3/2}(\alpha p_T)} \quad (30)$$

Fig. 3 show the application of this procedure to $(K^* + \bar{K}^*)/(K_S)$ and $\Sigma^*(1385)/\Lambda$. It is apparent that, while the presence of transverse flow makes sure these distributions depend on the freeze-out temperature, their shape allows the different freeze-out models to be differentiated from each other whatever the temperature is. If Hubble freezeout occurs, the two parameters will tend to coincide ($\frac{\partial t_f}{\partial r} = \alpha$). If the ansatz fitted in [7, 8] are correct and t_f is indeed independent on radius, β cancels out as well and eq. 29 will reduce to a particularly simple form

$$\frac{Y^*}{Y} = \left(\frac{g^*}{g} \right) \frac{I_0(\alpha p_T^*)}{I_0(\alpha p_T)} \quad (31)$$

These analytically simple forms are valid if the light particle Y has been corrected for feed-down from resonances, including Y^* . In other words, Eq. 31 and 29, as well as Fig. 3 require that decay products from reconstructed Y^* do not appear on the bottom of the ratio. Experiments usually [16, 17, 18, 19] do not do such feed-down corrections since it would increase both statistical and systematic error on the ratio, and indeed it is not always possible to do them. For instance, in case of the η'/η ratio (whose usefulness is discussed later in the paper), feed-down can not be accounted for by the experiment, since both particles are detected through the $\gamma\gamma$ channel [41, 42], while the dominant decay mode of the η' is the (undetectable) $\eta' \rightarrow \pi\pi\eta$.

Introducing the feed-down corrections into Eq. 27, one gets (assuming the resonance itself will not have any significant feed-down corrections to it, as is the case for all particles considered here)

$$\frac{Y^*}{Y} = \frac{g^* S(m_T, p_T^*, \alpha, \beta)}{g S(m_T, p_T, \alpha, \beta) + \sum_i g_i^* R(m_T, p_{Ti}^*, \alpha, \beta)} \quad (32)$$

Here, $S(m_T, p_T, \alpha, \beta)$ describes the directly produced particles and has the form given by eq. 23 and each term $R(m_T, p_{Ti}^*, \alpha, \beta)$ describes a feed-down contribution.

In the case of an incoherent many-particle system, such as the one we are dealing with, the dynamical (Matrix element) part of the decay amplitude factors out [43], and $R(m_T, p_{Ti}^*, \alpha, \beta)$ it will be given by integrating the original (statistical hadronization) distribution with a weight given by the phase space elements of the decay products. thus, for a generic $Y^* \rightarrow Y$ feed-down given by an N-body decay

$$R(p_\mu, \alpha, \beta) = \quad (33)$$

$$\int \prod_2^N \frac{d^3 p_i}{E_i} S(m_T^*, p_T^*, \alpha, \beta) \delta(p_\mu^* - p_\mu - \sum_2^N p_{i\mu})$$

where the integral is performed over the whole kinematically allowed region. If more than one feed-down occurs, Eq 33 can be used iteratively, with the LHS to be fed back to the RHS at each successive iteration.

In general, this expression can get very complicated, and Montecarlo integration becomes necessary. For most cases considered here, where there is one feed-down and two or three body decays, eq. 33 can be performed semi-analytically [10, 15, 20].

Fig. 4 shows the ratios, including feed-down for resonances, for $(K^{*0} + \bar{K}^{*0})/(all K_S)$, $\Sigma^*/(all \Lambda)$ and $\eta'/(all \eta)$. In the $\Sigma^*/(all \Lambda)$ case we omitted the feed-down from Ξ , or the ratio would depend strongly on the chemical potential. We did, however, include the $\phi \rightarrow K_S K_L$ feed-down, since it is a strong decay that can not so easily be corrected by experiment.

As one can see, correction for feed-down does make a large difference. In particular, the complicated resonance redistribution makes Fig. 4 less sensitive to freeze-out geometry, and less simple to analyze than Fig. 3. Because feed-down from particles with a different chemical composition, (such as $\phi \rightarrow K_S K_L$) can not always be corrected at the experimental level, some resonances ratios will also acquire a dependence on the chemical potentials. This is also true for ratios, such as $\eta'/(all \eta)$, of quark-antiquark states with different $s\bar{s}$ content. (in this paper, these chemical corrections were put to unity).

However, since a range of m_T distributions sufficient to extricate freeze-out temperature, flow and chemical factors is presently available, the m_T dependance of a few resonance's ratios might enable us to differentiate between the different freeze-out geometries, in particular between a fast blast-wave type model and Hubble.

The presence of a long Hadron gas rescattering phase can distort these distributions considerably: Of course, the global Y^*/Y ratio will be altered due to the depletion of the detectable resonances through the rescattering of their decay products. It's dependance on m_T , however, will also be affected in a non-trivial way, since faster (higher p_T) resonances will have a greater chance to emerge the fireball without decaying, thus avoiding the rescattering phase altogether.

Experimental signals have already been proposed for the existance of such a phase [14, 15]. At present there is no evidence that it plays a great role in particle distributions. Since the m_T dependance of Eq. 29 and 32 differs considerably, feed-down correction for some hyperons at the experimental level would provide a more stringent test for the effect of rescattering. (This could be feasible in case of the Σ^* and perhaps the K^* .) It would also help to differentiate between freeze-out models, since Eq. 29 is more sensitive to the form of Σ^μ

Since the existance, and the effect of rescattering are at present ambiguous, the optimum probes for freeze-out are the particles most unlikely to rescatter. For this reason, $\eta \rightarrow \gamma\gamma$ is particularly useful, since it's long lifetime and electromagnetic decay channel makes it very insensitive to post-hadronization dynamics. η mesons have been de-

tected at SPS energies through this channel [41, 42], and detectors such as PHENIX are capable of reconstructing the same decays at RHIC. Note that while η and η' have very different branching ratios, they have the same degeneracies and similar (very small) widths. This, together with their small chance to regenerate (the dominant decay mode of both the η and η' is three-body) makes them ideal probes for the analysis considered here.

In summary, we have presented an overview of the different statistical hadronization models used to fit heavy ion data. We analyzed in detail one of these differences, namely the structure of the emitting hypersurface at hadronization, and have shown that the different choices made of this hypersurface are a consequence of different assumptions about hadronization. We proposed the m_T

dependence of the resonance ratios as a probe for further analysis of this crucial aspect of statistical hadronization. and we hope that, as more spectra and resonance data becomes available, the situation will be further qualified.

Acknowledgments

Supported by a grant from the U.S. Department of Energy, DE-FG03-95ER40937. We thank Patricia Fachini and Zhangbu Xu, from the STAR collaboration, as well as Marcus Bleicher for fruitful discussions

[1] E. Fermi, *Prog. Theor. Phys.* **5** (1950) 570.

[2] I. Pomeranchuk, *Proc. USSR Academy of Sciences (in Russian)* **43** (1951) 889.

[3] R. Hagedorn, *Suppl. Nuovo Cimento* **2** (1965) 147.

[4] J. Rafelski and J. Letessier, arXiv:nucl-th/0209084.

[5] P. Braun-Munzinger, I. Heppe and J. Stachel, *Phys. Lett. B* **465**, 15 (1999).

[6] F. Becattini and G. Pettini, arXiv:hep-ph/0204340.

[7] J. M. Burward-Hoy for the PHENIX collaboration QM 2002 and proceedings

[8] M. Van Leeuwen for the NA49 collaboration QM 2002 and proceedings

[9] G. Torrieri and J. Rafelski, *New J. Phys.* **3**, 12 (2001) [arXiv:hep-ph/0012102].

[10] W. Broniowski and W. Florkowski, *Phys. Rev. Lett.* **87**, 272302 (2001) [arXiv:nucl-th/0106050].

[11] S. V. Akkelin, P. Braun-Munzinger and Y. M. Sinyukov, *Nucl. Phys. A* **710**, 439 (2002) [arXiv:nucl-th/0111050].

[12] D. Magestro, *J. Phys. G* **28**, 1745 (2002) [arXiv:hep-ph/0112178].

[13] C. Suire for the STAR collaboration QM 2002 and proceedings

[14] G. Torrieri and J. Rafelski, *J. Phys. G* **28**, 1911 (2002) [arXiv:hep-ph/0112195].

[15] G. Torrieri and J. Rafelski, *Phys. Lett. B* **509**, 239 (2001) [arXiv:hep-ph/0103149].

[16] P. Fachini [STAR Collaboration], arXiv:nucl-ex/0211001.

[17] G. Van Buren for the STAR collaboration QM 2002 and proceedings

[18] C. Markert [STAR Collaboration], *J. Phys. G* **28**, 1753 (2002).

[19] V. Friese [NA49 Collaboration], *Nucl. Phys. A* **698** (2002) 487.

[20] E. Schnedermann, J. Sollfrank and U. W. Heinz, *Phys. Rev. C* **48**, 2462 (1993) [arXiv:nucl-th/9307020].

[21] E. Schnedermann, J. Sollfrank and U. W. Heinz, TPR-92-29 *Lectures given at NATO Advanced Study Inst. on Particle Production in Highly Excited Matter, Ciocco, Italy, Jul 12-24, 1992*

[22] F. Cooper and G. Frye, *Phys. Rev. D* **10** (1974) 186

[23] K. A. Bugaev, *Nucl. Phys. A* **606**, 559 (1996) [arXiv:nucl-th/9906047].

[24] C. Anderlik *et al.*, *Phys. Rev. C* **59**, 3309 (1999) [arXiv:nucl-th/9806004].

[25] Jean Letessier and Johann Rafelski *Hadrons and Quark-Gluon Plasma* Cambridge monographs on particle physics, nuclear physics and cosmology Cambridge University Press

[26] D. Teaney, J. Lauret and E. V. Shuryak, arXiv:nucl-th/0110037.

[27] J. D. Bjorken, *Phys. Rev. D* **27**, 140 (1983).

[28] J. Letessier and J. Rafelski, *J. Phys. G* **28**, 183 (2002) [arXiv:hep-ph/0106151].

[29] J. Rafelski and J. Letessier, *Phys. Rev. Lett.* **85**, 4695 (2000) [arXiv:hep-ph/0006200].

[30] R. D. Pisarski, arXiv:nucl-th/0212015.

[31] A. Dumitru and R. D. Pisarski, *Nucl. Phys. A* **698**, 444 (2002) [arXiv:hep-ph/0102020].

[32] S. Pratt, QM 2002 and proceedings A. Dumitru and R. D. Pisarski, *Nucl. Phys. A* **698**, 444 (2002) [arXiv:hep-ph/0102020].

[33] A. Keranen, J. Manninen, L. P. Csernai and V. Magas, arXiv:nucl-th/0205019.

[34] B. Touschek, *Nuovo Cimento B* **58**, 295 (1968).

[35] R. Hagedorn, I. Montvay, and J. Rafelski CERN-TH-2605, Dec 1978, in: *Hadronic Matter at Extreme Energy Density*, pp49–148, N. Cabibbo and L. Sertorio, Edts. (Plenum Press, New York 1980).

[36] T. Susa [NA49 Collaboration], *Nucl. Phys. A* **698** (2002) 491.

[37] M. Gazdzicki [NA49 Collaboration], *Prepared for 30th International Workshop on Gross Properties of Nuclei and Nuclear Excitation: Hirschegg 2002: Ultrarelativistic Heavy Ion Collisions, Hirschegg, Austria, 13-19 Jan 2002*

[38] S. V. Afanasyev *et al.* [NA49 Collaboration], *J. Phys. G* **28**, 1761 (2002) [arXiv:nucl-ex/0201012].

[39] A. Olszewski *et al.* [PHOBOS Collaboration], *J. Phys. G* **28**, 1801 (2002).

[40] P. Staszek *et al.*, *Acta Phys. Polon. B* **33**, 1387 (2002).

[41] R. Albrecht *et al.* [WA80 Collaboration.], *Phys. Lett. B* **361**, 14 (1995) [arXiv:hep-ex/9507009].

[42] A. Lebedev *et al.* [WA80 Collaboration.], *Nucl. Phys. A* **566**, 355C (1994).

[43] J. Sollfrank, P. Koch and U. W. Heinz, *Prepared for 19th*

TABLE I: Freeze-Out hypersurfaces

Surface	Σ^μ	$E \frac{dN}{dp^3}$ ^a	reference
Constant t_f	$\left(\frac{\partial t_f}{\partial r} \right) = 0$	$\left(\begin{array}{c} t_f \\ \vec{r} \end{array} \right)$	$m_T K_1(\beta m_T) I_0(\alpha p_T)$ [7, 8, 13, 20, 33]
Hubble			
(constant τ_f)	$\tau_f \left(\begin{array}{c} \cosh(y_L) \cosh(y_T) \\ \sinh(y_T) \cos(\theta) \\ \sinh(y_T) \sin(\theta) \\ \sinh(y_L) \cosh(y_T) \end{array} \right)$	$m_T \cosh(y_T) I_0(\alpha p_T) K_1(\beta m_T) - p_T \sinh(y_T) I_1(\alpha p_T) K_0(\beta m_T)$	[10]
Boost-invariant Blast	$\left(\begin{array}{c} t_f(r) \cosh(y_L) \\ r \cos(\theta) \\ r \sin(\theta) \\ t_f(r) \sinh(y_L) \end{array} \right)$	$m_T I_0(\alpha p_T) K_1(\beta m_T) - p_T \frac{\partial t_f}{\partial r} I_1(\alpha p_T) K_0(\beta m_T)$	This paper , [10]
Spherical blast	$\left(\begin{array}{c} t_f \\ r \vec{e}_r \end{array} \right)$	$e^{-E/T} \sqrt{\frac{T}{p_T \sinh(y_T)}} (E I_{1/2}(\alpha p_T) - p_T \frac{\partial t}{\partial r} I_{3/2}(\alpha p_T))$	[9, 20]

$$^a \beta = \frac{\cosh(y_T)}{T}, \alpha = \frac{\sinh(y_T)}{T}$$

International Workshop on Gross Properties of Nuclei and Nuclear Excitations,

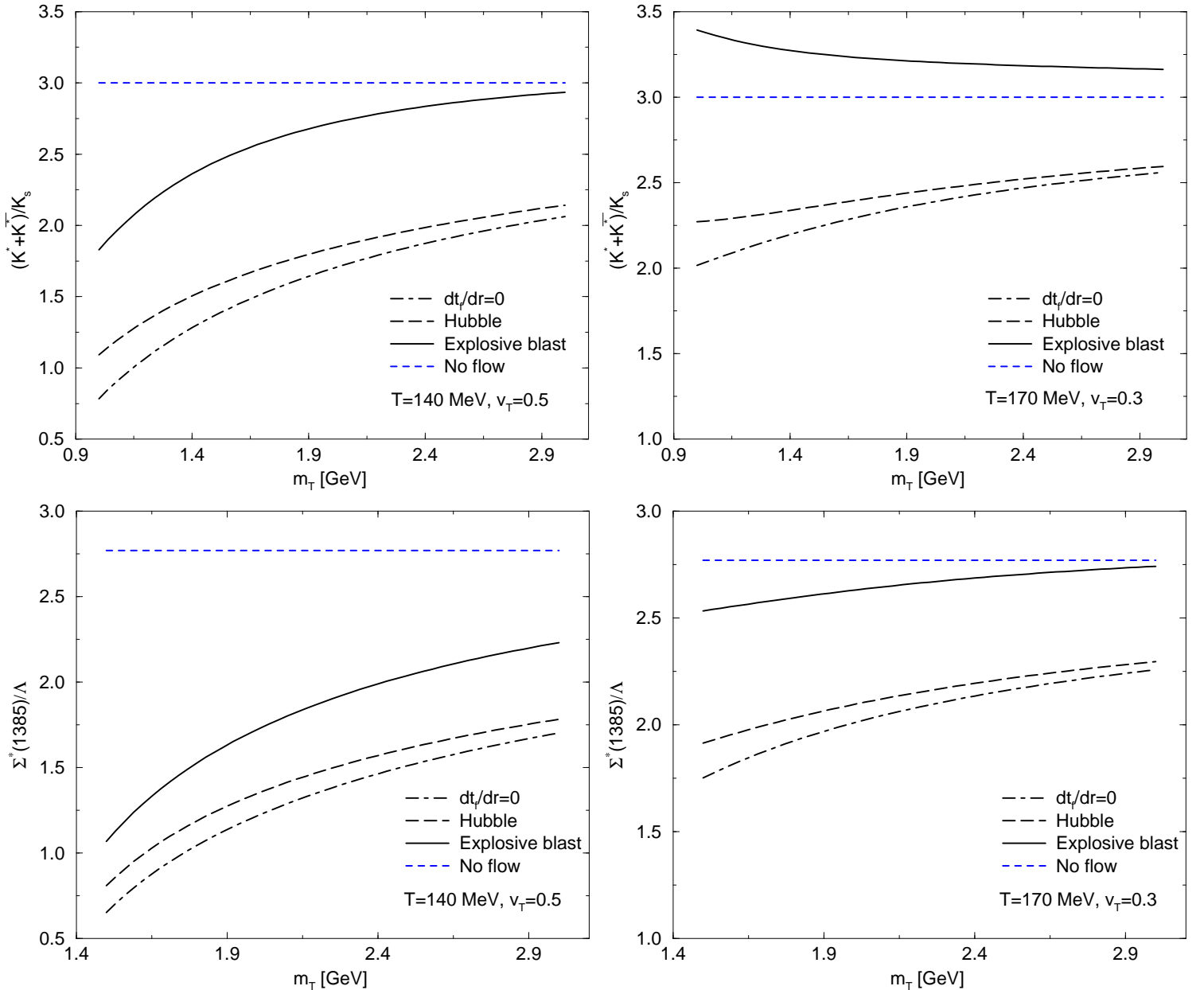


FIG. 3: Dependence of the K^*/K and Σ^*/Λ on the Freeze-out model .

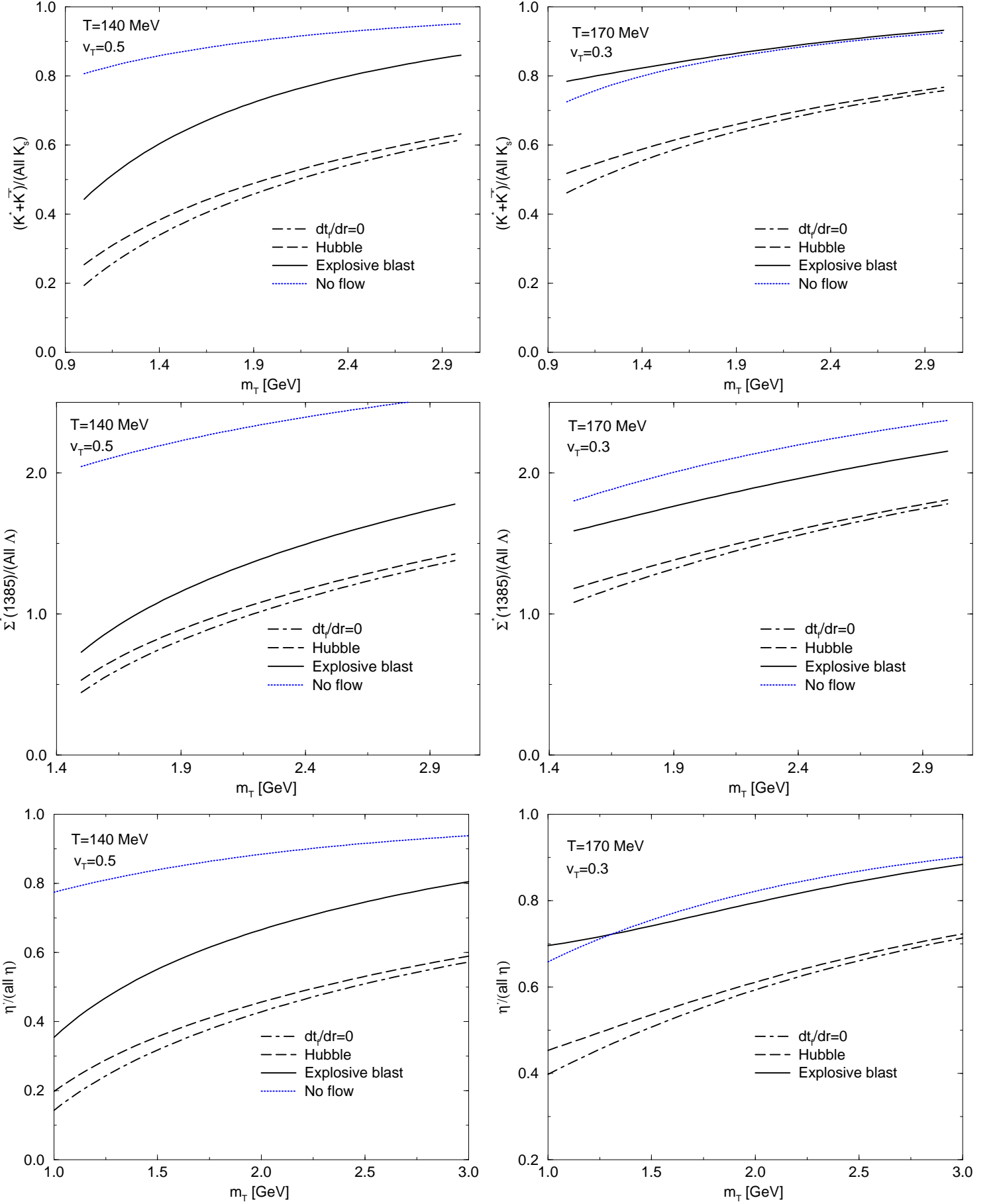


FIG. 4: $(K^* + \bar{K}^*)/(all\ K_s)$, $\Sigma^*(1385)/(all\ \Lambda)$ and $\eta'/(all\ \eta)$ ratios, including feed-down from resonances.